Stabilization of Zwitterions in Solution: Phosphinic and Phosphonic Acid GABA Analogues

Deborah L. Crittenden,[†,‡] Rohan J. Kumar,[†] Jane R. Hanrahan,[†] Mary Chebib,[†] and Meredith J. T. Jordan*[,‡]

Faculty of Pharmacy, University of Sydney, NSW 2006, Australia, and School of Chemistry, University of Sydney, NSW 2006, Australia

Received: March 10, 2005; In Final Form: July 17, 2005

The influence of treatment of electron correlation, size of basis set and choice of solvation model on the predicted stabilization of zwitterionic phosphinic and phosphonic acid γ-aminobutyric acid (GABA) analogues is investigated using ab initio molecular orbital methods and density functional theory. Density functional theory with the B3LYP functional and a composite basis set composed of the 6-31+G(2df) basis for phosphorus atoms and the 6-31+G(d,p) basis set for all other atoms is found to give an acceptable tradeoff between accuracy and computational expense. Either directly optimizing zwitterionic conformers within the conductor-like screening solvation model (COSMO) or pre-optimizing as dihydrates and then applying the COSMO solvation model give an acceptable treatment of solvation in terms of determining stable solvated structures, although directly optimizing within COSMO is simpler and less computationally expensive. With this protocol, cis-constrained phosphinic and phosphonic acid GABA analogues, which exhibit lower affinities for $GABA_C$ receptors, are found to possess only folded, intramolecularly hydrogen bonded low energy conformers. Trans-constrained analogues, on the other hand, exhibit higher affinities for $GABA_C$ receptors and are found to exist only as partially folded stable conformers. Conformationally flexible analogues can attain folded, partially folded or fully extended conformations and also have high biological activity. These results imply that the partially folded conformation is likely to be the most biologically active.

Introduction

GABA, γ-aminobutyric acid, is the major inhibitory neurotransmitter in the mammalian central nervous system.[1] It interacts with three major classes of GABA receptors, termed $GABA_A$, $GABA_B$ and $GABA_C$ receptors. $GABA_A$ and $GABA_C$ receptors are ionotropic or ligand-gated receptors,[2] whereas $GABA_B$ receptors are metabotropic or G-protein coupled receptors.[3] Historically, $GABA_A$[4] and $GABA_B$[3] receptors have long been identified as pharmacologically distinct receptor classes and it is therefore unsurprising that they have been the subject of intensive experimental and theoretical study. $GABA_C$ receptors, on the other hand, have only been discovered relatively recently,[5] and have been the subject of only a limited amount of experimental research.[6] The majority of experimental studies carried out to date have been in vitro studies to establish pharmacological profiles for this receptor class, as a lack of specific agonists for $GABA_C$ receptors has made it difficult to clearly determine their role in vivo.[6] The selective $GABA_C$ receptor antagonist (1,2,5,6-tetrahydropyridin-4-yl)methylphosphinic acid (TPMPA), however, has been shown to have significant biological effects, including (i) improving memory performance in rats and chicks,[7] (ii) affecting the sleep-wake behavior of rats,[8] (iii) inhibiting ammonia-induced apoptosis in hippocampal neurons[9] and (iv) regulating hormone release in the pituitary.[10] In general, phosphinic and phosphonic GABA analogues have been shown to be potent and selective $GABA_C$ receptor antagonists, and these compounds may be useful leads in the development of more specific $GABA_C$ ligands.[6,7,11−14] To date, however, no theoretical studies have been carried out to investigate the structure−activity relationships of these compounds at $GABA_C$ receptors, as a result of both insufficient experimental biological activity data and a lack of high-quality structural data.

Possessing both a basic amino functionality on one end of the molecule and an acidic phosphinic or phosphonic group on the other end, phosphinic and phosphonic acid GABA analogues can exist in either zwitterionic or nonzwitterionic forms, depending on the polarity of the surrounding environment. As the mammalian body is a predominantly aqueous environment, it is necessary to accurately account for solvent effects when determining biologically active structures.

The only set of previous calculations on phosphinic and phosphonic acid GABA analogues were carried out by Lorenzini et al., in the context of determining structures of $GABA_B$ receptor ligands.[15] In this work, a semiempirical method (PM3) was employed both to optimize the geometry of the compounds considered and for subsequent conformational exploration. However, given that these calculations were carried out using a method parametrized for neutral species and solvent effects were neglected, it is unlikely that the results provide accurate representations of the solution-phase structures.

Therefore, in this current work, we establish a computational protocol for accurately and efficiently modeling solvated zwitterionic phosphinic and phosphonic acid GABA analogues and then apply this protocol to generate high-quality structures for use in subsequent quantitative structure−activity relationship (QSAR) analysis. Further, we intend to model a broader range of phosphinic and phosphonic acid GABA analogues, as a large number of these compounds exhibit biological activity at $GABA_C$ receptors. The structures of the compounds under investigation here are illustrated in Figure 1 and their full

* Corresponding author. E-mail: m.jordan@chem.usyd.edu.au.
† Faculty of Pharmacy.
‡ School of Chemistry.

10.1021/jp051227p CCC: $30.25
Published on Web 08/25/2005

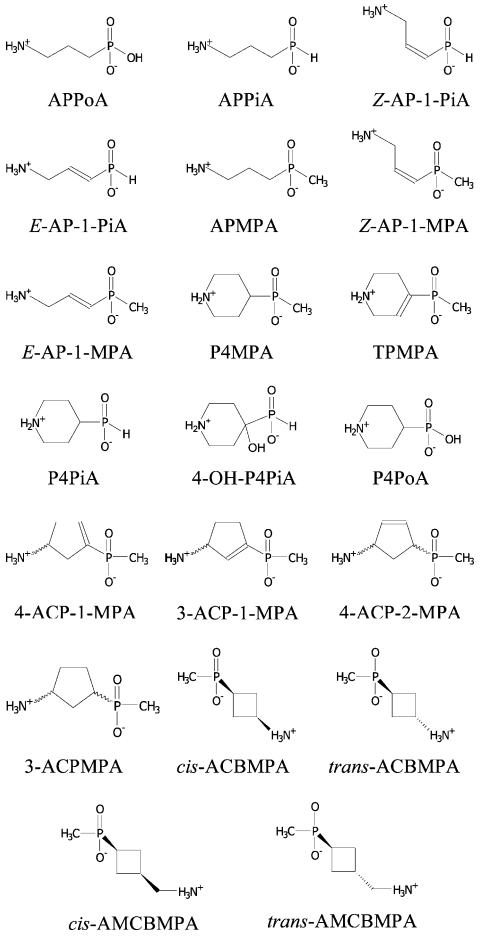

Figure 1. Line structures of phosphinic and phosphonic acid GABA analogues.

chemical names and abbreviations can be found in Table 1. These compounds have been chosen for investigation because they either have been or are in the process of being synthesized and characterized for biological activity at $GABA_C$ receptors.

Computational Methods

All basis sets used in this work are composite basis sets, composed of a larger basis with more polarization functions for the phosphorus atoms than the basis set used for the other atoms, following the recommendations of Haworth et al.[16] In the interests of brevity and clarity, we introduce here a notation to describe these composite basis sets. Throughout this paper, a composite basis set will be denoted using the abbreviation G(polarization functions on phosphorus)/(polarization functions on all other atoms) at the end of the basis set specification for Pople basis sets. For example, a composite basis with the 6-31+G(2df) basis set describing phosphorus atoms and the 6-31+G(d,p) basis set describing all other atoms would be denoted 6-31+G(2df)/(d,p).

TPMPA was used as a model system to establish an appropriate level of theory for determining the structures and relative energies of phosphinic and phosphonic acid GABA analogues. TPMPA was chosen because its conformational rigidity significantly reduces the number of stable conformations it can attain relative to its more conformationally flexible counterparts shown in Figure 1.

In this work, we have considered four different methods for incorporating aqueous solvent effects. The simplest model involved determining the stable gas-phase conformations then calculating solvation corrections at those geometries. This model will be referred to as "gas phase". Optimizing the geometries in a dielectric continuum instead of the gas phase provided a second, more sophisticated model. This model will be referred to as "bulk solvated". The final two models involved initially optimizing the conformers as dihydrates. Continuum solvation corrections were calculated both on the dihydrated system and on the isolated solute molecule with the explicit water molecules removed. These methods will subsequently be referred to as "dihydrated" and "dehydrated dihydrate", respectively. The relative energies of the conformers without the continuum solvation correction applied will be denoted ΔE_{int}, and the relative bulk solvated energies will be denoted ΔE_{solv}. The computational details of each method are described below.

Stable conformers of gas-phase TPMPA were determined by geometry optimization with subsequent rotation of all rotatable bonds and reoptimization from all identified local minima, using density functional theory with the B3LYP functional[19−21] and the 6-31+G(2df)/(d,p) basis.[22−27] The global minimum was then reoptimized either by substituting the basis set for a 6-311+G-(3df)/(d,p) basis[24−27] or by using second-order Møller−Plesset perturbation theory (MP2).[28−31]

Stable conformers on the solvated B3LYP/6-31+G(2df)/(d,p) TPMPA potential energy surface were found using the geometry optimization and conformational exploration procedure outlined

TABLE 1: Full Chemical Names and Abbreviations of the Compounds Studied

	abbreviation	full chemical name
1	APPoA	(3-aminopropyl)phosphonic acid
2	APPiA	(3-aminopropyl)phosphinic acid
3	*Z*-AP-1-PiA	(*Z*-3-aminopropen-1-yl)phosphinic acid
4	*E*-AP-1-PiA	(*E*-3-aminopropen-1-yl)phosphinic acid
5	APMPA	(3-aminopropyl)methylphosphinic acid
6	*Z*-AP-1-MPA	(*Z*-3-aminopropen-1-yl)methylphosphinic acid
7	*E*-AP-1-MPA	(*E*-3-aminopropen-1-yl)methylphosphinic acid
8	P4MPA	piperidin-4-ylmethylphosphinic acid
9	TPMPA	(1,2,5,6-tetrahydropyridin-4-yl)phosphinic acid
10	P4PiA	piperidin-4-ylphosphinic acid
11	4-OH−P4PiA	(4-hydroxypiperidin-4-yl)phosphinic acid
12	P4PoA	piperidin-4-ylphosphonic acid
13	4-ACP-1-MPA	(4-amino-1-cyclopenten-1-yl)methylphosphinic acid
14	3-ACP-1-MPA	(3-amino-1-cyclopenten-1-yl)methylphosphinic acid
15	4-ACP-2-MPA	(4-amino-1-cyclopenten-2-yl)methylphosphinic acid
16	3-ACPMPA	(3-aminocyclopentanyl)methylphosphinic acid
17	*cis*-ACBMPA	*cis*-(3-amino-1-cyclobutane)methylphosphinic acid
18	*trans*-ACBMPA	*trans*-(3-amino-1-cyclobutane)methylphosphinic acid
19	*cis*-AMCBMPA	*cis*-(3-(aminomethyl)-1-cyclobutyl)methylphosphinic acid
20	*trans*-AMCBMPA	*trans*-(3-(aminomethyl)-1-cyclobutyl)methylphosphinic acid

TABLE 2: Geometric Data for the Lowest Energy Gas Phase Nonzwitterionic and Bulk Solvated Zwitterionic TPMPA Conformers at Different Levels of ab Initio Theory[a]

gas phase	N−C−C−C (deg)	C−C−C−P (deg)	C−C−P−O (deg)	C−C−P−OH (deg)	C−C−P−CH_3 (deg)	RMS (Å)
B3LYP/6-31+G(2df)/(d,p)	−12.9	177.8	−6.4	−131.4	122.9	0.0
	48.5	164.2	173.0	47.9	−57.7	
B3LYP/6-311+G(3df)/(d,p)	−12.5	177.8	−5.8	−131.2	123.1	0.0107
	48.4	164.1	173.5	48.2	−57.6	
MP2/6-31+G(2df)/(d,p)	−14.0	177.7	−8.0	−133.5	121.4	0.0361
	50.4	163.9	171.4	45.9	−59.2	
bulk solvated	**N−C−C−C**	**C−C−C−P**	**C−C−P−O**	**C−C−P−O**	**C−C−P−CH_3**	**RMS (Å)**
B3LYP/6-31+G(2df)/(d,p)	−12.3	−179.5	2.8	131.6	−113.2	0.0
	46.9	161.7	−175.6	−46.8	68.4	
B3LYP/6-311+G(3df)/(d,p)	−12.3	−179.3	2.2	131.0	−113.8	0.0098
	46.8	161.5	−176.0	−47.1	68.0	
MP2/6-31+G(2df)/(d,p)	−12.8	−179.8	2.2	131.2	−113.9	0.0332
	48.4	161.5	−176.3	−47.3	67.7	

[a] Representative dihedral angles and root-mean-squared deviation in atomic position with respect to the B3LYP/6-31+G(2df)/(d,p) geometry as fit by all-atom least-squares superposition. Where two sets of dihedral angles are listed, these correspond to angles measured around opposite sides of the cyclohexene ring.

above, within the conductor-like screening solvation model (COSMO)[32,33] with a dielectric constant of $\epsilon = 78.39$ chosen to mimic the dielectric constant of water and thus incorporate aqueous solvation effects. Again, the global minimum energy conformer was reoptimized at B3LYP/6-311+G(3df)/(d,p) and MP2/6-31+G(2df)/(d,p) within the COSMO reaction field.

All identified stable gas-phase and solvated TPMPA conformers were reoptimized as dihydrates at B3LYP/6-31+G(2df)/(d,p). Solvation corrections to the energy of both the dihydrated and "dehydrated dihydrate" conformers were calculated using the COSMO model.

Single point energy calculations were performed on the stable gas-phase, bulk solvated, dihydrated and "dehydrated" dihydrate TPMPA conformers at B3LYP/6-31+G(2df)/(d,p), B3LYP/6-31+G(3df)/(d,p), B3LYP/6-311+G(3df)/(d,p), B3LYP/6-311++G(3df)/(d,p) and MP2/6-31+G(2df)/(d,p). Again, bulk solvation effects were accounted for by application of the COSMO continuum solvation model.

As TPMPA does not possess an intramolecular hydrogen bond due to its conformational rigidity, further benchmarking calculations were carried out on (3-aminopropyl)phosphonic acid (APPoA) and (3-aminopropyl)phosphinic acid (APPiA) to explore the neutral-zwitterionic tautomeric equilibrium in aqueous solution. Geometry optimizations were carried out at B3LYP/6-31+G(2df)/(d,p) within the COSMO solvation model, starting from nonzwitterionic, intramolecularly hydrogen-bonded structures.

On the basis of these benchmarking calculations, stable conformers of the other compounds shown in Figure 1 were determined by geometry optimization at B3LYP/6-31+G(2df)/(d,p) within the COSMO solvation model. Further low-energy aqueous-phase rotamers were found by rotation about rotatable bonds and reoptimization from the identified local minima.

Figures were generated using GaussView1.0.[17] In all figures presented in this paper, the atoms are represented as grayscale spheres. The hydrogen atoms are white, the carbon atoms are light gray, the nitrogen atoms are black, the oxygen atoms are dark gray and the phosphorus atoms are intermediate gray.

All calculations reported here were carried out using the Gaussian 03 program suite[18] on the computing facilities at the School of Chemistry, University of Sydney, and at the Australian Partnership of Advanced Computing National Facility, based at the Australian National University.

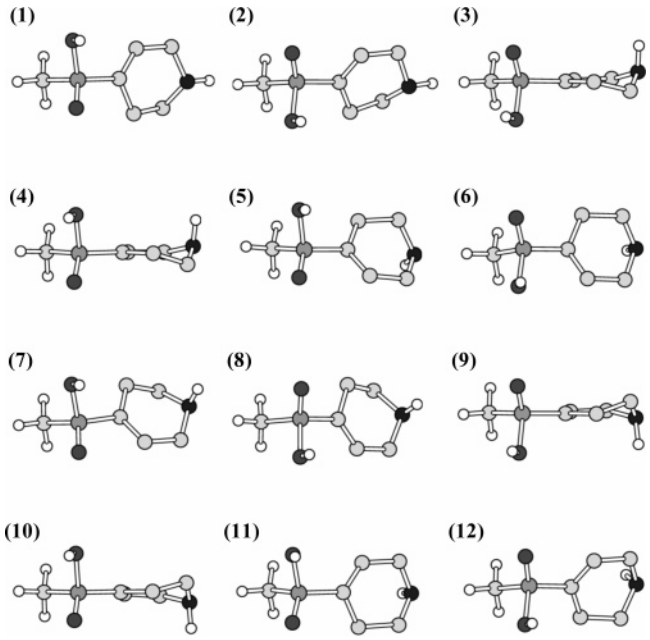

Figure 2. Low-energy nonzwitterionic TPMPA conformers optimized at B3LYP/6-31+G(2df)/(d,p) in the gas phase. For clarity, only terminal hydrogen atoms have been displayed.

Results and Discussion

Geometrical data for the global minimum energy gas-phase nonzwitterionic and bulk solvated zwitterionic TPMPA conformers are presented in Table 2. The root-mean-squared deviation in atomic positions, presented in Table 2, was generated by least-squares superposition of the B3LYP/6-311+G(3df)/(d,p) and MP2/6-31+G(2df)/(d,p) geometries upon the template B3LYP/6-31+G(2df)/(d,p) global minimum energy TPMPA structure. From Table 2, we observe that the root-mean-squared deviation in atomic position is less for the B3LYP/6-311+G(3df)/(d,p) optimized geometry than for the MP2/6-31+G(2df)/(d,p) optimized geometry. This implies that increasing the size of the basis set has less effect on the geometry than changing the treatment of electron correlation. However, even the largest root-mean-squared value of 0.0332 Å for the deviation of the MP2/6-31+G(2df)/(d) from the B3LYP/G-31+G(2df)/(d,p) bulk solvated conformer is relatively small. It can also be observed that the dihedral angle profile does not change significantly with an increase in basis set size or change in treatment of electron correlation, with a largest change of

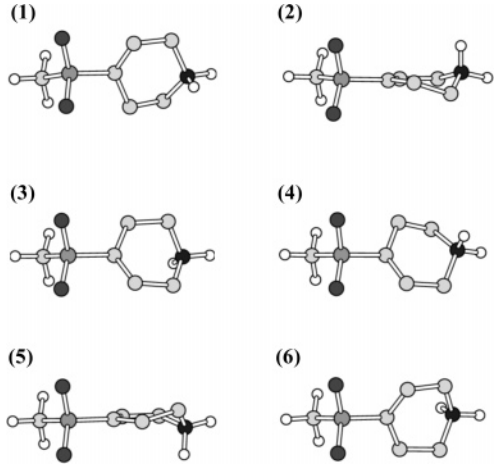

Figure 3. Low-energy zwitterionic TPMPA conformers optimized at B3LYP/6-31+G(2df)/(d,p) in the COSMO reaction field ($\epsilon = 78.39$). For clarity, only terminal hydrogen atoms have been displayed.

2.6° for the C−C−P−O dihedral of the minimum energy gas-phase conformer. In the context of using these geometries for subsequent quantitative structure−activity relationship analysis, these changes are sufficiently small that they can be considered negligible. Therefore, the combination of B3LYP as the electronic structure method with the 6-31+G(2df)/(d,p) basis set represents an acceptable compromise between accuracy and computational expense for obtaining geometrical data.

To assess the influence of level of ab initio theory and treatment of solvation on the relative energies, it was first necessary to locate all stable TPMPA conformers. These conformers were obtained by optimization in the gas phase, optimization within COSMO and optimization as an explicitly dihydrated complex. The twelve stable nonzwitterionic gas-phase conformers are illustrated in Figure 2 and the six stable bulk solvated zwitterionic conformers are illustrated in Figure 3. The geometries of the stable neutral and zwitterionic TPMPA conformers were independent of the solvation model used in the geometry optimization process; all solvation models identified neutral and zwitterionic structures similar to those shown in Figures 2 and 3. Therefore, structures obtained using other solvation models are not illustrated here but may be obtained as Supporting Information.

The stable gas-phase conformers illustrated in Figure 2 are related to one another by migration of the carboxylate-bound proton from one oxygen atom to the other, rotation about the carbon−phosphorus bond and ring flipping. Conformers 1−6 and 7−12 are ring-flip isomers of one another. Conformers 1 and 2, 3 and 4, 5 and 6 are related by proton migration. Accordingly, conformer pairs 7−8, 9−10 and 11−12 are also related by proton migration. Within each subset of ring-flip isomers, the odd-numbered conformers are related by rotation about the carbon−phosphorus bond, as are the even-numbered conformers. Zwitterionic TPMPA possesses only half as many stable conformers as nonzwitterionic TPMPA, as the phosphinic acid group is deprotonated and therefore both oxygen atoms are equivalent. Again, the full set of six stable conformers can be divided into two subsets (1−3 and 4−6) that are related by ring-flipping. Within each subset, the three identified stable conformers result from rotation about the carbon−phosphorus bond. All TPMPA conformers, nonzwitterionic and zwitterionic, can be classified as "extended" conformations, with a long

TABLE 3: Relative Energies of Gas Phase, Bulk Solvated, and Dihydrated TPMPA Conformers, at Different Levels of ab Initio Theory[a]

	gas phase		bulk solvated		dihydrate		"dehydrated" dihydrate	
	ΔE_{int}	ΔE_{solv}	ΔE_{int}	ΔE_{solv}	ΔE_{int}	ΔE_{solv}	ΔE_{int}	ΔE_{solv}
				B3LYP/6-31+G(2df)/(d,p)				
nonzwitterionic (1)	3.9	2.8	4.2	2.8	6.2	21.5	5.7	6.3
nonzwitterionic (2)	0.0	0.0	0.0	0.0	0.0	0.0	0.0	0.0
nonzwitterionic (3)	6.7	5.9	7.1	6.9	29.8	46.2	0.7	2.5
nonzwitterionic (4)	6.3	5.8	8.6	6.5	14.1	6.5	15.6	9.6
nonzwitterionic (5)	0.5	0.4	1.0	0.0	28.9	43.4	−2.7	1.0
nonzwitterionic (6)	3.8	3.1	7.4	6.9	24.1	14.4	23.6	15.5
zwitterionic (1)	149.2	0.4	162.4	−15.0	67.9	−7.5	148.9	−8.2
zwitterionic (2)	150.5	−1.1	161.1	−12.3	70.6	−6.4	150.6	−7.3
zwitterionic (3)	151.6	−4.5	162.5	−15.3	114.6	26.5	149.5	−4.7
				B3LYP/6-311+G(3df)/(d,p)				
nonzwitterionic (1)	3.7	2.7	3.8	2.5	6.8	22.0	6.0	6.9
nonzwitterionic (2)	0.0	0.0	0.0	0.0	0.0	0.0	0.0	0.0
nonzwitterionic (3)	6.3	5.9	6.5	6.7	28.8	45.8	0.9	2.7
nonzwitterionic (4)	5.9	5.8	6.3	6.3	12.9	5.6	14.1	8.8
nonzwitterionic (5)	0.0	0.5	0.4	0.0	28.0	42.8	−2.3	1.3
nonzwitterionic (6)	3.3	3.2	6.7	6.5	22.7	13.1	22.1	14.5
zwitterionic (1)	156.6	8.0	170.2	−6.8	72.1	−3.5	157.0	0.0
zwitterionic (2)	158.5	6.4	169.1	−4.2	74.2	−3.1	159.5	0.6
zwitterionic (3)	159.6	3.0	170.1	−7.2	120.5	31.8	156.4	2.9
				MP2/6-31+G(2df)/(d,p)				
nonzwitterionic (1)	4.0	2.9	4.3	2.8	2.5	18.1	5.1	5.9
nonzwitterionic (2)	0.0	0.0	0.0	0.0	0.0	0.0	0.0	0.0
nonzwitterionic (3)	8.3	7.5	8.9	8.7	33.9	49.2	1.7	3.9
nonzwitterionic (4)	8.0	7.6	8.7	8.2	16.4	8.3	17.8	11.9
nonzwitterionic (5)	0.8	1.1	1.5	0.7	32.7	46.1	−1.9	2.1
nonzwitterionic (6)	4.4	4.3	8.8	8.5	23.3	13.5	24.7	16.8
zwitterionic (1)	139.0	−12.8	151.6	−28.1	65.2	−14.2	138.6	−21.1
zwitterionic (2)	143.6	−13.0	154.5	−23.7	70.7	−11.5	143.2	−19.1
zwitterionic (3)	141.9	−17.5	152.2	−28.2	103.0	11.8	140.1	−16.8

[a] Relative gas phase energies are denoted ΔE_{int} and relative solvated energies are denoted ΔE_{Solv}. All energies are reported in kJ/mol and no zero-point corrections are included.

phosphorus−nitrogen distance, relative to other phosphinic and phosphonic acid GABA analogues which can adopt folded, intramolecularly hydrogen-bonded conformations.

The results presented in Table 3 illustrate the influence of changing the treatment of electron correlation in the electronic structure method, changing the size of basis set and using different solvation models on the relative energies of the nonzwitterionic TPMPA conformers 1−6 and zwitterionic conformers 1−3. As the ring-flip isomers of these conformers had identical energies, the energies of nonzwitterionic conformers 7−12 and 4−6 were not recalculated. Although the effects of treatment of electron correlation, size of basis set and choice of solvation model are not completely independent, they are only weakly interdependent and therefore will be discussed separately.

Comparison of the B3LYP/6-31+G(2df)/(d,p) and B3LYP/6-311+G(3df)/(d,p) results from Table 3 indicates that the relative stabilities of nonzwitterionic species are insensitive to basis set size. However, using a smaller basis set tends to overestimate the stability of the gas-phase, bulk solvated and "dehydrated dihydrate" zwitterionic conformers by around 8 kJ/mol. This effect is less pronounced for the energies of the dihydrated zwitterions relative to their dehydrated counterparts; in this case, the energy difference is only approximately 4 kJ/mol. It is also interesting to note that this effect is constant, irrespective of the solvation status of the system. That is, the difference between the gas-phase relative energies (ΔE_{int}) of the zwitterionic conformers is approximately the same as the difference between the solvation-corrected relative energies (ΔE_{solv}). Calculations were also carried out at B3LYP/6-31+G(3df)/(d,p) and B3LYP/6-311++G(3df)/(d,p), but these results were similar to the B3LYP/6-311+G(3df)/(d,p) results and are not included here. These data may be obtained in the Supporting Information.

The influence of the treatment of electron correlation by the ab initio or density functional method on the relative energies of the zwitterionic and nonzwitterionic TPMPA conformers can be determined by comparison of the B3LYP/6-31+G(2df)/(d,p) and MP2/6-31+G(2df)/(d,p) results from Table 3. From these results, we observe that B3LYP tends to underestimate the stability of the zwitterionic conformers relative to MP2, and the magnitude of this effect exhibits no clear dependence on either the method used to optimize the geometries or the solvation status of the system. This effect was also observed for GABA[34] and arises because of the larger dipole moments predicted at MP2. The maximum difference of 14.8 kJ/mol was observed for the solvation-corrected energy of dihydrated zwitterion conformer 3. The mean absolute difference, averaged over all zwitterionic conformers irrespective of optimization method or solvation status, was found to be 9.8 kJ/mol.

Overall, the B3LYP/6-31+G(2df)/(d,p) method tends to overestimate the stability of the zwitterionic TPMPA conformers by an average of around 8 kJ/mol due to basis set deficiencies, while simultaneously underestimating the stabilities by an average of approximately 10 kJ/mol relative to MP2, which includes a more systematic treatment of electron correlation effects. Fortuitously, these errors are approximately additive[35] and therefore cancel to give an overall average underestimate of the stability of approximately 2 kJ/mol. An estimate of the maximum error of this approach for TPMPA was obtained by adding the difference between the B3LYP/6-31+G(2df)/(d,p) results and the B3LYP/6-311+G(3df)/(d,p) results to the difference between the B3LYP/6-31+G(2df)/(d,p) and MP2/6-31+G(2df)/(d,p) results for each conformer. The maximum error was found to be 9.5 kJ/mol, for dihydrated zwitterionic conformer 3. Therefore, the B3LYP/6-31+G(2df)/(d,p) method represents a suitable method for determining solution-phase structures and energies of solvated zwitterionic phosphinic and phosphonic acid GABA analogues.

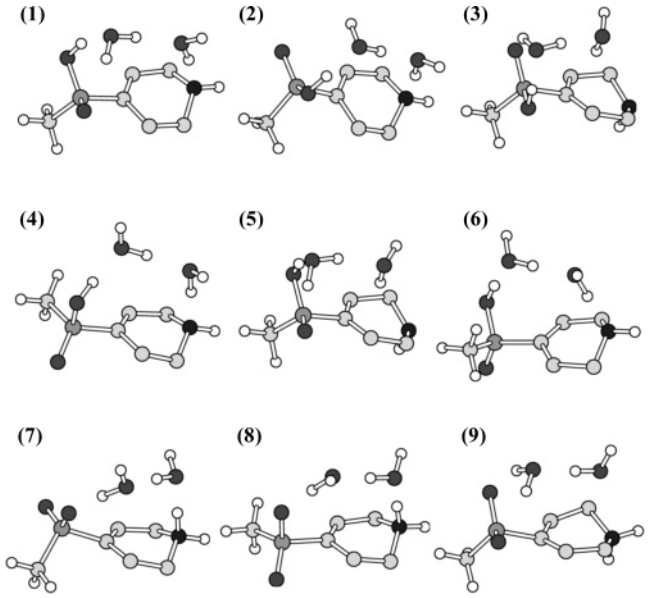

Figure 4. Low-energy nonzwitterionic (1−6) and zwitterionic (7−9) TPMPA conformers optimized as dihydrates at B3LYP/6-31+G(2df)/(d,p). For clarity, only terminal hydrogen atoms have been displayed.

The influence of different solvation models on the relative energies of zwitterionic and nonzwitterionic TPMPA conformers can also be ascertained from the data presented in Table 3. For simplicity, only the B3LYP/6-31+G(2df)/(d,p) data will be discussed here, as B3LYP/6-31+G(2df)/(d,p) gives similar trends in relative energies to B3LYP/6-311+G(3df)/(d,p) and MP2/6-31+G(2df)/(d,p).

From Table 3, we observe that the gas-phase energies (ΔE_{int}) of the zwitterionic TPMPA conformers are significantly higher than those of the nonzwitterionic conformers, irrespective of how the energies were obtained—whether through optimization in the gas phase, in a continuum solvation model, as dihydrates or as "dehydrated" dihydrates. The fact that the dihydrated zwitterionic conformers are also significantly higher in energy than the nonzwitterionic dihydrates suggests that two water molecules are insufficient to stabilize the zwitterionic form of phosphinic and phosphonic acid GABA analogues. These results are in contrast with previous studies on GABA,[34] which suggest that two water molecules are sufficient to stabilize the zwitterionic form, such that the nonzwitterionic and zwitterionic forms are at least approximately isoenergetic.

Unlike the gas-phase internal energy differences, the relative solvation-corrected energies, ΔE_{solv}, of TPMPA fall within a relatively narrow range for all conformers when isolated molecules are placed within a bulk continuum, as occurs in the gas phase, bulk solvated and "dehydrated dihydrate" models. In general, the zwitterionic conformers are significantly lower in energy than the nonzwitterionic conformers, except in the case of conformers obtained by gas phase optimization, where the zwitterionic conformers are approximately isoenergetic with the nonzwitterionic conformers. Although the gas-phase optimized geometries are qualitatively similar to the solvated optimized geometries, the gas-phase geometries do not correspond to minima on the solvated PES. Consequently, this approach would not be expected to provide a realistic estimate of the relative energies of the solvated conformers. The results obtained from the TPMPA conformers optimized in a continuum solvation model or the "dehydrated" dihydrates are expected

to possess a more realistic potential energy profile for the bulk solvated isolated molecules. The most complicated solvation model considered here is known as the supermolecule approach, which involves calculating the solvation energy by embedding the optimized dihydrate in a bulk continuum. The relative energies obtained according to this approach exhibit a surprisingly large range of values. In particular, nonzwitterionic TPMPA conformers 3 and 5 (Figure 2) and zwitterionic conformer 3 (Figure 3) are significantly higher in energy than the other conformers. This effect is also observed in the relative energies of the gas phase dihydrates. This discrepancy can be explained by examining the optimized TPMPA dihydrate geometries, illustrated in Figure 4. From this figure, we observe that the majority of the optimized dihydrates possess three intermolecular hydrogen bonds; one between the phosphinic acid group and a water molecule, one between the two water molecules and one between the second water molecule and the amino group. The exception to this trend occurs for nonzwitterionic conformers 3 and 5 and zwitterionic conformer 3, where the amino group is orientated away from the phosphinic acid group and two water molecules are insufficient to bridge between the amino and phosphinic acid termini. Therefore, these systems possess only two intermolecular hydrogen bonds: one between the phosphinic acid group and a water molecule and the other between the two water molecules. The relative destabilization of these three conformers can be considered an artifact of only using two water molecules to model short-range solvent effects. Given sufficient water molecules to model explicit solute−solvent interactions, nonzwitterionic TPMPA conformers 3 and 5 would be expected to exhibit stabilities similar to those of the other nonzwitterionic conformers. Similarly, the relative energy of zwitterionic TPMPA conformer 3 would be expected to decrease to more resemble the energies of the other zwitterionic conformers.

Overall, all three solvation models considered here (bulk solvated, solvated dihydrate and solvated "dehydrated" dihydrate) indicate that zwitterionic conformers are more stable in solution than the nonzwitterionic conformers. These methods predicted relative stabilities ranging from 4.7 to 15.3 kJ/mol. Of these three approaches, optimizing in a continuum solvation model was the most straightforward and computationally efficient and we have therefore used this method to obtain geometrical and energetic data for the other phosphinic and phosphonic acid GABA analogues shown in Figure 1.

To confirm that the zwitterionic form is preferred in aqueous solution, even for conformationally flexible compounds, solution phase geometry optimizations of nonzwitterionic, intramolecularly hydrogen bonded forms of APPiA and APPoA were carried out. During the geometry optimization, the proton migrated from the carboxylate group to the amino group, resulting in the identification of the zwitterionic structure as the global minimum on the potential energy surface for both compounds. This provides a convincing proof that phosphinic and phosphonic acid GABA analogues exist primarily as zwitterions in aqueous solution.

Energetic and selected geometric data for the phosphinic and phosphonic acid GABA analogues shown in Figure 1 are presented in Table 4, and all identified zwitterionic minimum energy structures are illustrated in Figures 3 and 5−21. From Table 4, we observe that the relative energies of the stable conformers fall within a narrow range, at most 29.6 kJ/mol from the global minimum, for all compounds considered. Given the approximate nature of both the level of ab initio theory and the treatment of solvation, all conformers of each compound can be considered approximately isoenergetic in aqueous solution. The coordinate data for all optimized geometries are available as Supporting Information. The structural features of the stable aqueous phase zwitterionic conformers of each compound will be discussed in more detail below, with the exception of TPMPA, which was used to benchmark the methods.

APPoA. The nine identified stable zwitterionic APPoA conformers are illustrated in Figure 5. Conformer 1 was identified directly by optimization within the COSMO dielectric continuum solvation model; the other conformers were obtained by rotation about the C1−C2 and C2−C3 bonds. Conformers 1, 3, 8 and 9 are folded, intramolecularly hydrogen-bonded structures, and conformers 2, 4, 6 and 7 are partially folded structures that possess no intramolecular hydrogen bond. Conformer 5 represents a fully extended conformation. An additional two sets of 9 low-energy conformers are accessible by rotation about the carbon−phosphorus bond in 120° increments. However, in the interest of conserving computational resources, refinement of these structures by geometry optimization was not carried out. This is justified on the basis that the unoptimized rotamers are expected to be sufficiently similar to reoptimized rotamers for subsequent quantitative structure−activity analysis.

APPiA. The stable zwitterionic APPiA conformers (Figure 6) are analogous to the stable APPoA conformers, differing only in the substitution of a proton for the phosphorus-bound hydroxide group. Accordingly, the analysis of the APPoA conformers given above also holds for the APPiA conformers. The relative energies of the APPoA and APPiA conformers also follow the same trends.

***Z*-AP-1-PiA.** The geometries corresponding to stable zwitterionic structures on the bulk solvated *Z*-AP-1-PiA potential energy surface are illustrated in Figure 7. All four local minima were found to correspond to folded, intramolecularly hydrogen-bonded conformers. These four conformers were identified by geometry optimization to give conformer 1 and subsequent conformational exploration by rotation about the C1−C2 and C3−P bonds. These two bonds are the only two rotatable bonds that do not lead to minima that are equivalent by nuclear permutation symmetry, as rotation about the C1−N bond does. Therefore, the conformers thus identified represent the full set of local minima on the bulk solvated *Z*-AP-1-PiA potential energy surface. This full set of local minima can be divided into two subsets of conformers that are enantiomers of one another. Conformers 1 and 2 are enantiomers of conformers 3 and 4, respectively.

***E*-AP-1-PiA.** The stable solution phase zwitterionic *E*-AP-1-PiA conformers are depicted in Figure 8. These six conformers represent the full set of local minima, as the conformational exploration protocol involved rotation about all rotatable bonds, as outlined for *Z*-AP-1-PiA above. All six conformers can be classified as partially folded. Conformers 1, 3 and 4 are enantiomers of compounds 2, 6 and 5, respectively.

APMPA. Like APPiA, the stable zwitterionic APMPA conformers (Figure 9) are analogous to the stable APPoA conformers, although in the case of APMPA a methyl group is substituted for the phosphorus-bound hydroxide group of APPoA. Again, the discussion of the different conformations of APPoA is applicable to the APMPA conformers, and the relative energies of the APMPA and APPoA conformers are similar.

***Z*-AP-1-MPA.** The stable zwitterionic *Z*-AP-1-MPA conformers (Figure 10) are analogous to the stable *Z*-AP-1-PiA conformers, differing only in the substitution of a methyl group for the phosphorus-bound hydrogen. Accordingly, the analysis

TABLE 4: Energetic and Selected Geometric Data for the Stable Aqueous Phase Conformers of a Range of Phosphinic and Phosphonic Acid GABA Analogues[a]

analogue name (conformer no.)	N−C−C−C (deg)	C−C−C−P (deg)	C−C−P−O (deg)	C−C−P−O (deg)	C−C−P−X (deg)	C−C−C−C (deg)	ΔE_{solv} (kJ/mol)
APPoA (1)	−44.1	−42.7	71.8	−59.7	−173.8		8.7
APPoA (2)	−66.3	−175.6	65.2	−67.3	−179.3		23.9
APPoA (3)	−75.0	77.6	70.0	−61.3	−172.3		0.0
APPoA (4)	−179.8	−71.0	68.0	−64.5	−176.3		24.2
APPoA (5)	−179.5	178.6	65.6	−66.9	−178.9		20.0
APPoA (6)	178.6	70.4	61.7	−70.8	177.1		24.2
APPoA (7)	66.3	174.5	66.5	−66.1	−178.1		24.0
APPoA (8)	43.3	43.9	60.7	−70.9	178.5		27.4
APPoA (9)	75.0	−77.1	61.6	−69.6	172.7		0.0
APPiA (1)	−43.4	−42.1	71.4	−59.6	−176.0		9.8
APPiA (2)	−65.8	−175.0	−66.4	65.4	179.5		26.7
APPiA (3)	−74.2	77.1	−60.8	69.8	−173.8		0.0
APPiA (4)	−178.4	−70.9	69.5	−62.3	−176.2		26.8
APPiA (5)	−179.8	−179.9	−63.3	68.4	−177.4		22.4
APPiA (6)	179.1	71.9	−68.4	63.4	177.4		26.8
APPiA (7)	65.4	173.7	−66.2	65.5	179.7		26.7
APPiA (8)	42.3	43.1	−70.6	60.4	176.9		9.8
APPiA (9)	74.2	−76.7	60.9	−69.7	173.9		0.0
Z-AP-1-PiA (1)	−54.5	−2.5	26.0	−105.0	140.2		0.0
Z-AP-1-PiA (2)	42.1	−1.0	−8.2	−139.2	105.6		0.7
Z-AP-1-PiA (3)	54.7	2.5	−26.4	104.6	−140.6		0.0
Z-AP-1-PiA (4)	−51.5	0.6	8.5	139.5	−105.4		0.5
E-AP-1-PiA (1)	−118.3	−178.3	−117.8	111.9	−2.9		0.0
E-AP-1-PiA (2)	116.7	178.6	−113.3	116.4	1.5		0.0
E-AP-1-PiA (3)	−118.2	179.5	2.4	−129.1	117.4		3.2
E-AP-1-PiA (4)	120.1	176.4	3.1	−128.5	118.0		3.2
E-AP-1-PiA (5)	−122.6	−175.9	−5.4	126.2	−120.3		3.2
E-AP-1-PiA (6)	118.5	−179.5	−2.1	129.4	−117.2		3.1
APMPA (1)	−74.7	77.2	66.6	−61.1	−175.6		0.0
APMPA (2)	−43.1	−42.5	71.4	−56.7	−174.6		9.8
APMPA (3)	−66.5	−176.4	65.0	−63.8	−179.5		28.8
APMPA (4)	−179.2	−71.1	67.8	−61.1	−176.5		29.5
APMPA (5)	−179.8	180.0	64.3	−64.6	179.9		24.6
APMPA (6)	179.4	73.3	65.4	−63.4	−179.2		29.6
APMPA (7)	65.9	176.4	66.4	−62.5	−178.1		28.8
APMPA (8)	41.9	44.1	56.3	−71.7	174.3		9.8
APMPA (9)	74.6	−77.0	61.3	−66.4	175.8		0.0
Z-AP-1-MPA (1)	−51.8	1.3	9.4	137.6	−106.0		0.2
Z-AP-1-MPA (2)	−53.0	−3.1	23.8	−104.4	139.3		0.0
Z-AP-1-MPA (3)	48.8	−1.7	−4.5	−132.8	110.9		0.1
Z-AP-1-MPA (4)	51.7	3.2	−22.1	106.0	−137.8		0.0
E-AP-1-MPA (1)	−116.6	−178.7	−118.8	114.7	−2.2		1.7
E-AP-1-MPA (2)	115.9	178.7	−116.5	116.9	0.3		1.7
E-AP-1-MPA (3)	−118.3	179.1	−126.2	2.4	119.0		0.0
E-AP-1-MPA (4)	119.9	175.5	−123.7	5.1	121.5		0.2
E-AP-1-MPA (5)	−120.7	−175.6	125.1	−3.8	−120.3		0.2
E-AP-1-MPA (6)	118.8	−179.3	126.3	−2.4	−118.9		0.2
P4MPA (1)	−55.2	−76.5	73.3	−55.5	−170.3		8.0
	55.1	74.9	−53.0	178.2	63.4		
P4MPA (2)	−54.8	−75.4	51.4	−179.7	−65.0		8.3
	55.0	76.8	−75.1	53.8	168.6		
P4MPA (3)	−52.8	−88.3	−52.9	−179.6	63.6		18.6
	53.0	88.2	173.7	47.0	−69.8		
P4MPA (4)	−55.6	−178.8	57.7	−71.0	172.7		0.0
	55.1	−179.4	−178.5	52.8	−63.5		
P4MPA (5)	−55.4	179.1	176.7	−54.8	61.5		0.2
	55.4	179.3	−59.6	68.9	−174.8		
P4MPA (6)	−55.4	−175.6	50.6	178.3	−65.6		0.6
	55.2	175.2	177.7	−54.6	61.5		
TPMPA (1)	−13.4	177.0	−5.5	−134.4	110.2		0.3
	45.8	166.2	172.7	43.8	−71.6		
TPMPA (2)	−13.0	178.5	117.9	−115.2	1.4		3.0
	46.6	164.2	−62.4	64.5	−178.9		
TPMPA (3)	−12.3	−179.5	2.8	131.6	−133.2		0.0
	46.9	161.7	−175.6	−46.8	68.4		
TPMPA (4)	13.2	−176.5	4.5	133.4	111.3		0.1
	−46.1	−166.5	−173.3	−44.4	70.8		
TPMPA (5)	13.3	−179.3	−112.1	121.2	4.5		3.0
	−46.3	−163.8	67.7	−59.2	−175.7		

TABLE 4: Cont'd

analogue name (conformer no.)	N−C−C−C (deg)	C−C−C−P (deg)	C−C−P−O (deg)	C−C−P−O (deg)	C−C−P−X (deg)	C−C−C−C (deg)	ΔE_{solv} (kJ/mol)
TPMPA (6)	12.7	179.2	−1.8	−130.6	114.2		0.1
	−46.6	−161.7	176.5	47.7	−67.5		
P4PiA (1)	−54.5	−77.4	70.3	−61.9	−175.5		7.0
	54.2	77.7	−56.9	170.9	57.3		
P4PiA (2)	−55.3	−179.2	64.6	−67.4	178.4		0.0
	55.5	179.0	−171.0	57.1	−57.1		
4-OH-P4PiA (1)	−54.3	−76.1	−69.0	62.6	177.7		6.2
	54.1	76.5	166.0	−62.4	52.7		
4-OH-P4PiA (2)	−55.5	177.1	68.2	−63.4	−178.2		0.0
	55.7	−177.4	−170.0	58.5	−56.4		
P4PoA (1)	−54.9	−77.4	−60.8	71.6	−175.9		6.2
	54.4	76.8	172.4	−55.1	57.4		
P4PoA (2)	−55.7	179.6	50.7	−176.7	−64.6		0.0
	55.1	−178.5	−73.6	58.9	171.1		
cis-ACBMPA	97.2	−102.9	−73.1	54.2	169.4		0.0
	−97.3	100.6	−172.9	−45.6	69.5		
trans-ACBMPA	−136.5	−102.0	−72.6	55.9	172.1		25.2
	136.5	100.1	−173.6	−45.1	71.1		
cis-AMCBMPA (1)	−173.9	−112.4	−71.7	56.8	172.9	110.4	23.1
	−73.3	111.0	−174.7	−46.1	69.9	−107.2	
cis-AMCBMPA (2)	73.4	−112.7	−72.7	55.9	171.8	107.6	23.0
	174.1	111.0	−175.6	−47.0	68.9	−110.7	
cis-AMCBMPA (3)	−69.5	−116.4	−76.0	50.9	166.2	118.9	0.0
	36.5	112.9	−178.6	−51.7	63.6	−117.5	
trans-AMCBMPA (1)	−177.1	102.9	−41.8	−170.5	74.3	136.4	21.0
	−72.5	−104.8	59.9	−68.8	176.0	−133.7	
trans-AMCBMPA (2)	−54.9	103.0	−45.7	178.9	70.4	141.2	28.4
	55.7	−104.5	56.3	−72.5	172.4	−141.1	
trans-AMCBMPA (3)	177.0	−104.8	−72.1	56.6	172.7	−136.3	21.8
	72.4	103.1	−173.8	−45.1	71.0	133.5	
(*R*)-4-ACP-1-MPA	95.9	−168.6	64.1	−63.0	−179.5		0.0
(*S*)-4-ACP-1-MPA	−96.2	168.9	−64.3	62.8	179.3		0.0
(*R*)-3-ACP-1-MPA	108.8	−178.8	115.5	−117.3	−1.0		0.0
(*S*)-3-ACP-1-MPA	−109.4	179.1	115.2	−117.5	−1.1		0.0
(1*R*,4*R*)-4-ACP-2-MPA	136.2	106.8	70.0	−58.2	−174.9		30.2
(1*S*,4*S*)-4-ACP-2-MPA	−134.3	−108.6	−68.9	59.4	176.0		30.0
(1*R*,4*S*)-4-ACP-2-MPA	−91.9	97.3	72.9	−54.1	−169.7		0.0
(1*S*,4*R*)-4-ACP-2-MPA	91.9	−97.4	−72.9	54.1	169.8		0.0
(1*R*,4*R*)-3-ACPMPA	151.0	121.8	−62.8	65.7	−179.0		27.8
(1*S*,4*S*)-3-ACPMPA	−154.3	−116.0	64.1	−64.4	−179.8		28.1
(1*R*,4*S*)-3-ACPMPA	−82.2	100.8	−63.2	63.9	−178.4		0.0
(1*S*,4*R*)-3-ACPMPA	82.2	−100.8	63.1	−64.0	178.3		0.0

[a] X = H for phosphinic acids (denoted by Pi in name of compound), OH for phosphonic acid (denoted by Po in name of compound), and CH_3 for methylphosphinic acid (denoted MPA in name of compound).

of the *Z*-AP-1-PiA conformers given above can be generalized to explain the *Z*-AP-1-MPA conformers. The relative energies of the *Z*-AP-1-PiA and *Z*-AP-1-MPA conformers also follow the same trends.

***E*-AP-1-MPA.** The stable zwitterionic *E*-AP-1-MPA conformers (Figure 11) are analogous to the stable *E*-AP-1-PiA conformers, differing only in the substitution of a methyl group for the phosphorus-bound hydrogen. Accordingly, the analysis of the *E*-AP-1-PiA conformers given above also holds for the *E*-AP-1-MPA conformers. The relative energies of the *E*-AP-1-PiA and *E*-AP-1-MPA conformers are also similar.

P4PMA. All six stable zwitterionic conformers on the bulk solvated P4MPA potential energy surface are illustrated in Figure 12. Conformers 1, 2 and 3 correspond to conformations with the methylphosphinic acid group in an axial position relative to the piperidine ring whereas conformers 4, 5 and 6 correspond to conformations with the methylphosphinic acid group in an equatorial position relative to the piperidine ring. For each subset of stable conformers (axial or equatorial) all three conformers are related by rotation about the carbon−phosphorus bond. Additionally, conformers 1 and 2 and conformers 4 and 5 are ring-flip isomers of one another. All six identified P4MPA conformers can be categorized as partially folded.

P4PiA. Only two of the six stable zwitterionic P4PiA conformers are shown in Figure 13. Conformer 1 corresponds to a conformation with the phosphinic acid group in the axial position relative to the piperidine ring, whereas conformer 2 corresponds to a conformation with the phosphinic acid group in an equatorial position relative to the piperidine ring. Two other local minima can be accessed for each identified conformer by rotation about the carbon−phosphorus bond in 120° increments, although refinement of the structures of these conformers by geometry optimization has not been carried out here, as discussed in the APPoA section above. Analogous to the results obtained for P4MPA, all six stable P4PiA conformers can be categorized as partially folded structures.

4-OH-P4PiA. The stable zwitterionic 4-OH-P4PiA conformers (Figure 14) are analogous to the stable P4PiA conformers,

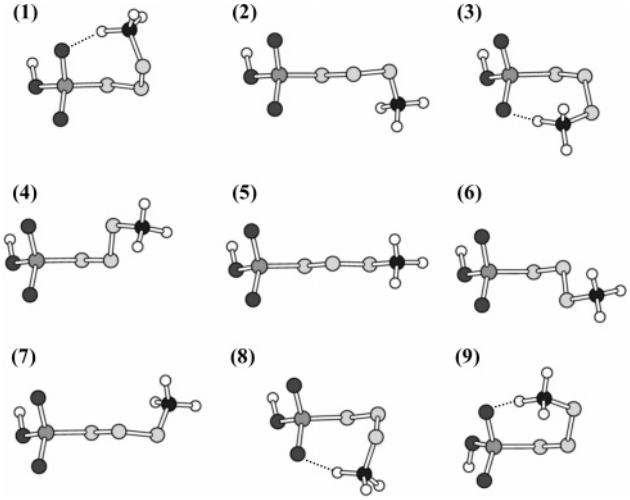

Figure 5. Low-energy B3LYP/6-31+G(2df)/(d,p) bulk solvated zwitterionic APPoA conformers. For clarity, only terminal hydrogen atoms have been displayed. Intramolecular hydrogen bonds are indicated as dotted lines.

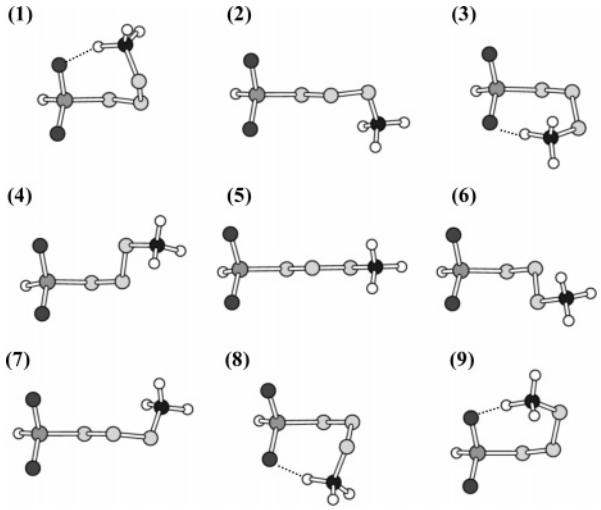

Figure 6. Low-energy B3LYP/6-31+G(2df)/(d,p) bulk solvated zwitterionic APPiA conformers. For clarity, only terminal hydrogen atoms have been displayed. Intramolecular hydrogen bonds are indicated as dotted lines.

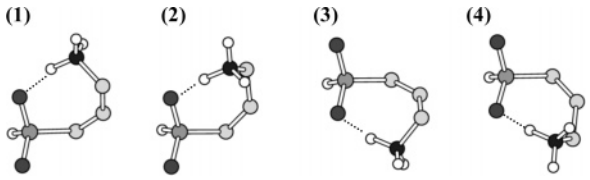

Figure 7. Low-energy B3LYP/6-31+G(2df)/(d,p) bulk solvated zwitterionic *Z*-AP-1-PiA conformers. For clarity, only terminal hydrogen atoms have been displayed. Intramolecular hydrogen bonds are indicated as dotted lines.

differing only in the addition of a hydroxyl group onto the 4 position of the piperidine ring. Accordingly, the analysis of the P4PiA conformers given above is relevant for the 4-OH-P4PiA conformers. The relative energies of the 4-OH-P4PiA and P4PiA conformers are also similar.

P4PoA. The stable zwitterionic P4PoA conformers shown in Figure 15 are analogous to the stable P4PiA conformers, differing only in the addition of a hydroxyl group onto the 4 position of the piperidine ring. Accordingly, the analysis of the P4PiA conformers given above also holds for the P4PoA

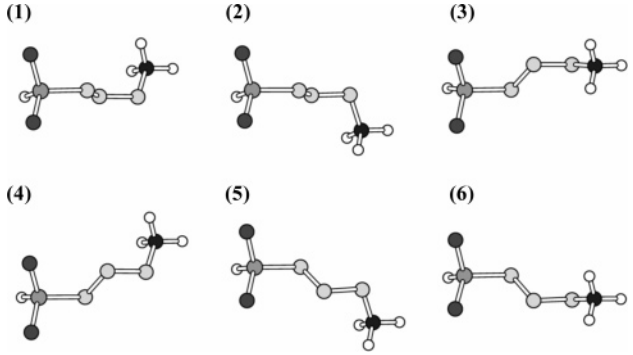

Figure 8. Low-energy B3LYP/6-31+G(2df)/(d,p) bulk solvated zwitterionic *E*-AP-1-PiA conformers. For clarity, only terminal hydrogen atoms have been displayed.

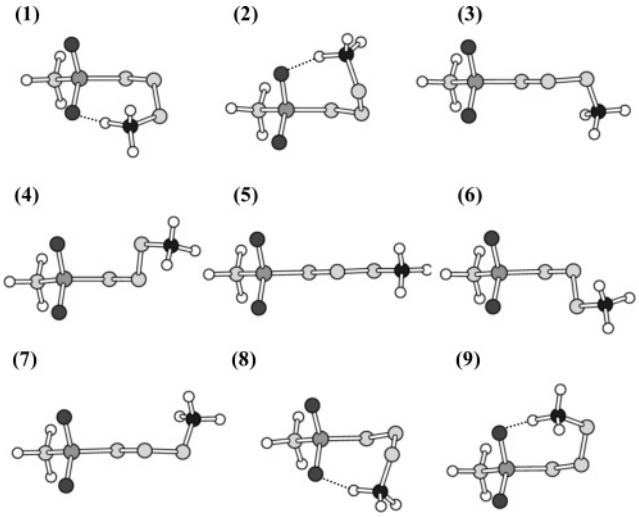

Figure 9. Low-energy B3LYP/6-31+G(2df)/(d,p) bulk solvated zwitterionic APMPA conformers. For clarity, only terminal hydrogen atoms have been displayed. Intramolecular hydrogen bonds are indicated as dotted lines.

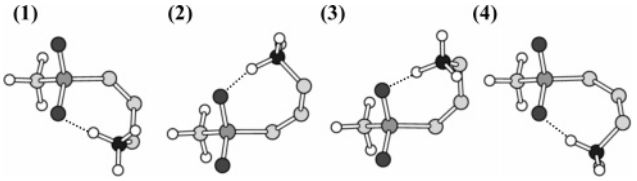

Figure 10. Low-energy B3LYP/6-31+G(2df)/(d,p) bulk solvated zwitterionic *Z*-AP-1-MPA conformers. For clarity, only terminal hydrogen atoms have been displayed. Intramolecular hydrogen bonds are indicated as dotted lines.

conformers. The relative energies of the P4PoA conformers also follow the same trends as the relative energies of the P4PiA conformers.

4-ACP-1-MPA. The lowest energy zwitterionic conformers of (*R*)-4-ACP-1-MPA and (*S*)-4-ACP-1-MPA are illustrated in Figure 16. Two more stable isomers of each enantiomer are accessible by rotation about the carbon−phosphorus bond in 120° increments, although refinement of the structures of these conformers by geometry optimization has not been carried out here, as discussed in the APPoA section above. All three stable conformers of each enantiomer can be classified as partially folded structures.

3-ACP-1-MPA. Like 4-ACP-1-MPA, 3-ACP-1-MPA possesses both an (*R*)- and (*S*)-enantiomer, and the lowest energy (*R*)- and (*S*)-zwitterionic enantiomers are shown in Figure 17. Again, two more conformers of each enantiomer are accessible

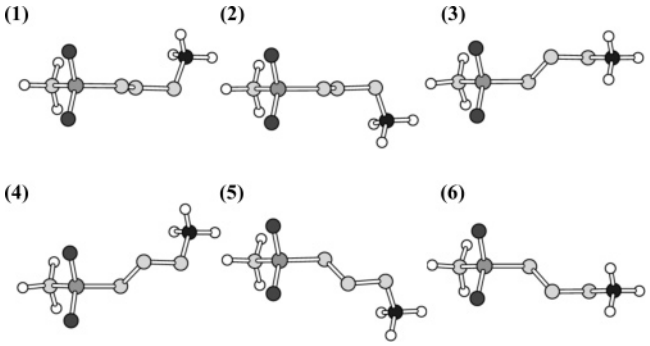

Figure 11. Low-energy B3LYP/6-31+G(2df)/(d,p) bulk solvated zwitterionic *E*-AP-1-MPA conformers. For clarity, only terminal hydrogen atoms have been displayed.

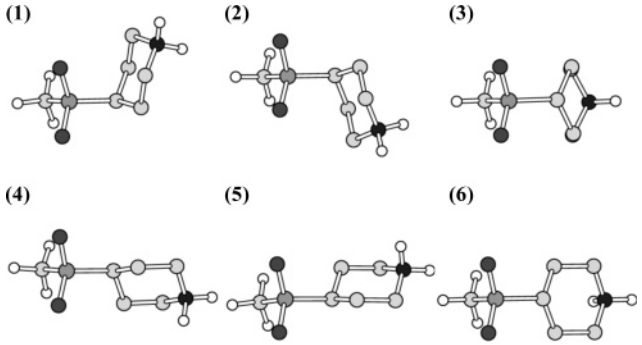

Figure 12. Low-energy B3LYP/6-31+G(2df)/(d,p) bulk solvated zwitterionic P4MPA conformers. For clarity, only terminal hydrogen atoms have been displayed.

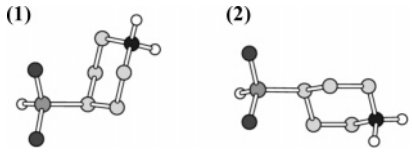

Figure 13. Low-energy B3LYP/6-31+G(2df)/(d,p) bulk solvated zwitterionic P4PiA conformers. For clarity, only terminal hydrogen atoms have been displayed.

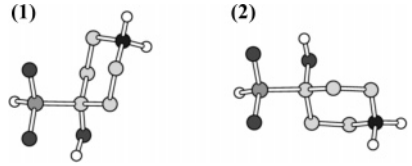

Figure 14. Low-energy B3LYP/6-31+G(2df)/(d,p) bulk solvated zwitterionic 4-OH-P4PiA conformers. For clarity, only terminal hydrogen atoms have been displayed.

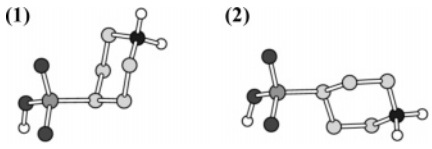

Figure 15. Low-energy B3LYP/6-31+G(2df)/(d,p) bulk solvated zwitterionic P4PoA conformers. For clarity, only terminal hydrogen atoms have been displayed.

by rotation about the carbon−phosphorus bond, although the structures are not subsequently refined. All three conformers of both the (*R*)- and (*S*)-enantiomers are partially folded.

4-ACP-2-MPA. As a consequence of having two stereocenters (one at the 1-position and one at the 3-position of the cyclopentene ring) 4-ACP-2-MPA possesses four enantiomers. The two cis-constrained enantiomers are (*R*,*S*)- and (*S*,*R*)-4-ACP-2-MPA and the two trans-constrained enantiomers are

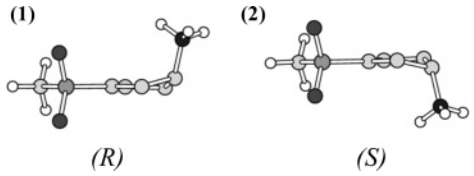

Figure 16. Low-energy zwitterionic 4-ACP-1-MPA conformers optimized at B3LYP/6-31+G(2df)/(d,p) in the COSMO reaction field (ϵ = 78.39). For clarity, only terminal hydrogen atoms have been displayed.

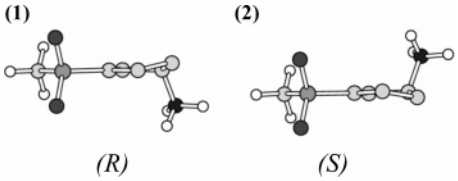

Figure 17. Low-energy zwitterionic 3-ACP-1-MPA conformers optimized at B3LYP/6-31+G(2df)/(d,p) in the COSMO reaction field (ϵ = 78.39). For clarity, only terminal hydrogen atoms have been displayed.

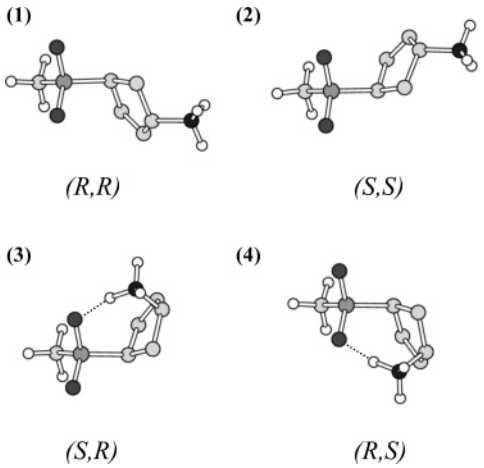

Figure 18. Low-energy zwitterionic 4-ACP-2-MPA conformers optimized at B3LYP/6-31+G(2df)/(d,p) in the COSMO reaction field (ϵ = 78.39). For clarity, only terminal hydrogen atoms have been displayed. Intramolecular hydrogen bonds are indicated as dotted lines.

(*R*,*R*)- and (*S*,*S*)-4-ACP-2-MPA. The minimum energy zwitterionic conformers of each of these four enantiomers are illustrated in Figure 18. Two more stable conformers are accessible for each of the trans-constrained enantiomers by rotation about the carbon−phosphorus bond in 120° increments. All six trans-constrained conformers attain partially folded conformations. Only a single extra low-energy conformer is accessible for each of the cis-constrained enantiomers, corresponding to rotation about the carbon−phosphorus bond by 120° such that the oxygen atom originally uninvolved in hydrogen bonding replaces the hydrogen atom originally involved in hydrogen bonding. All four cis-constrained conformers attain folded, intramolecularly hydrogen bonded conformations. Again, refinement of the structures obtained by rotation about the carbon−phosphorus bond has not been carried out here, as discussed in the APPoA section above.

3-ACPMPA. The stable zwitterionic 3-ACPMPA conformers shown in Figure 19 are analogous to the stable 4-ACP-2-MPA conformers, differing only in the saturation of the double bond in the 2 position of the cyclopentene ring. Accordingly, the analysis of the 4-ACP-2-MPA conformers given above also holds for the 3-ACPMPA conformers. The relative energies of the 3-ACPMPA conformers also follow the same trends as the relative energies of the 4-ACP-2-MPA conformers.

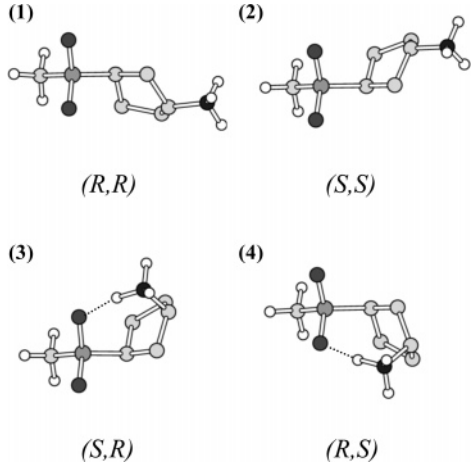

Figure 19. Low-energy zwitterionic 3-ACPMPA conformers optimized at B3LYP/6-31+G(2df)/(d,p) in the COSMO reaction field ($\epsilon = 78.39$). For clarity, only terminal hydrogen atoms have been displayed. Intramolecular hydrogen bonds are indicated as dotted lines.

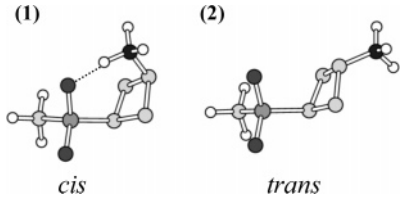

Figure 20. Low-energy zwitterionic *cis*- and *trans*-ACBMPA conformers optimized at B3LYP/6-31+G(2df)/(d,p) in the COSMO reaction field ($\epsilon = 78.39$). For clarity, only terminal hydrogen atoms have been displayed. Intramolecular hydrogen bonds are indicated as dotted lines.

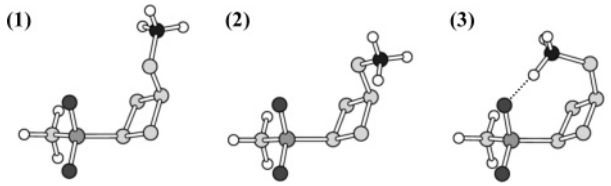

Figure 21. Low-energy zwitterionic B3LYP/6-31+G(2df)/(d,p) bulk solvated *cis*-AMCBMPA conformers. For clarity, only terminal hydrogen atoms have been displayed. Intramolecular hydrogen bonds are indicated as dotted lines.

***cis*-ACBMPA.** The lowest energy zwitterionic *cis*-ACBMPA conformer is illustrated in Figure 20, and another stable conformer is accessible by rotation about the carbon−phosphorus bond by 120° such that the original non hydrogen-bonded atom replaces the hydrogen bonded atom. Both conformers can be classified as folded, intramolecularly hydrogen bonded structures.

***trans*-ACBMPA.** One stable zwitterionic *trans*-ACBMPA conformer is shown in Figure 20, and two more stable conformers are accessible by rotation about the carbon−phosphorus bond in increments of 120°. All three stable conformers thus identified fall into the category of partially folded zwitterionic structures.

***cis*-AMCBMPA.** Three stable zwitterionic *cis*-AMCBMPA conformers are depicted in Figure 21. Conformer 1 was identified directly by optimization within the COSMO dielectric continuum solvation model; the other conformers were obtained by rotation about the C3−C4 bond. Conformers 1 and 2 exhibit partially folded conformations, whereas conformer 3 exists in a folded, intramolecularly hydrogen bonded form. two more stable partially folded conformers are accessible from conformers 1 and 2 by rotation about the carbon−phosphorus bond in 120° increments, whereas only one extra stable folded conformer is accessible from conformer 3, analogous to other cis-constrained compounds. Again, the structures of these compounds were not further refined here, as justified in the discussion of compound APPoA, above.

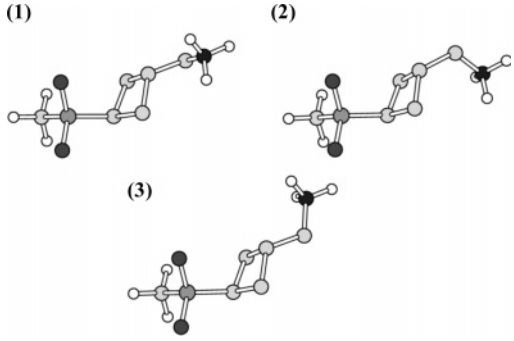

Figure 22. Low-energy zwitterionic B3LYP/6-31+G(2df)/(d,p) bulk solvated *trans*-AMCBMPA conformers. For clarity, only terminal hydrogen atoms have been displayed.

TABLE 5: Biological Activity Data for Selected Phosphinic and Phosphonic Acid GABA Analogues

compound name	IC_{50} (μM)	K_B (μM)	data from ref
APPiA	2.47 ± 0.04	3.2 ± 1.0	11
Z-AP-1-PiA	> 100		11
E-AP-1-PiA	7.7 ± 0.7	15.5 ± 1.7	11
APMPA	0.75 ± 0.07	0.58 ± 0.14	11
Z-AP-1-MPA	38.9 ± 4.9		11
E-AP-1-MPA	5.5 ± 1.2	8.6 ± 1.6	11
P4MPA		4.2	7
TPMPA		2.1	12
TPMPA		2.0 ± 0.4	11
P4PiA		2	14
4-OH−P4PiA		15	14
P4PoA		51	14

***trans*-AMCBMPA.** Three stable zwitterionic *trans*-AMCBMPA conformers are illustrated in Figure 22. As for *cis*-AMCBMPA, these structures were generated by conformational exploration involving rotation about the C3−C4 bond. Two more sets of three stable conformers are accessible by rotation about the carbon−phosphorus bond in 120° increments. All nine stable conformers on the solvated *trans*-AMCBMPA potential energy surface exhibit partially folded conformations.

Qualitative Structure−Activity Relationship Analysis. All existing biological activity data[7,11−14] for the compounds modeled here are summarized in Table 5. From this table, we observe that the cis-constrained compounds *Z*-AP-1-PiA and *Z*-AP-1-MPA have higher IC_{50} values at the $GABA_C$ receptor than the trans-constrained and conformationally flexible analogues. As the IC_{50} value is the concentration of drug required to inhibit 50% of a submaximal biological response, a higher IC_{50} value means that more drug is required because the compound has a lower affinity for the receptor. The only phosphonic acid analogue considered here, P4PoA, possesses a higher IC_{50} value than the phosphinic acid analogues. This suggests that both cis-constrained and phosphonic acid analogues have lower affinities for the agonist/competitive antagonist binding site. As the cis-constrained compounds were found to possess only folded, intramolecularly hydrogen-bonded structures, this suggests that such structures do not fit optimally into the $GABA_C$ receptor binding site. The trans-constrained compounds, on the other hand, attained only partially folded conformations, and the conformationally flexible APPiA and APMPA can attain folded, partially folded and fully extended conformations. Both the trans-constrained and conformationally flexible phosphinic acid

GABA analogues also exhibit relatively low IC_{50} values, implying that these compounds have a higher affinity for the $GABA_C$ receptor binding site. This suggests that the $GABA_C$ binding site preferentially accommodates partially folded or fully extended conformations. The fact that the majority of the compounds considered attain the partially folded conformation suggests that this conformation may be the biologically active structural motif, although the fully extended conformation cannot be excluded. This is in agreement with previous studies on conformationally restricted GABA analogues.[36] These studies suggest that compounds that can attain either fully extended or partially folded conformations are more active at $GABA_C$ receptors than compounds that exist exclusively in folded, intramolecularly hydrogen-bonded conformations.

Conclusions

Modeling solvated zwitterions using B3LYP/6-31+G(2df)/(d,p) and directly optimizing the structures within the COSMO dielectric continuum solvation model was found to provide an acceptable tradeoff between accuracy and computational expense. Phosphinic and phosphonic acid GABA analogues constrained in a cis-configuration were found to possess only folded, intramolecularly hydrogen bonded stable conformers. Analogues constrained in a trans configuration were found to be exclusively partially folded, whereas conformationally flexible analogues possessed stable folded, partially folded and fully extended conformers. As cis-constrained compounds have a lower affinity than trans-constrained or conformationally flexible compounds for the $GABA_C$ receptor binding site, it is postulated that the biologically active conformation must be either partially folded or fully extended. Overall, this work represents a systematic and accurate ab initio investigation into the solution phase structure of phosphinic and phosphonic acid GABA analogues.[36] Although this has enabled preliminary conclusions about the putative three-dimensional structure necessary for optimal binding to $GABA_C$ receptors, the real advantage of this work is that it provides a high-quality starting point for future quantitative structure−activity relationship analysis. This will, in turn, assist in the design and development of novel agents that selectively target $GABA_C$ receptors.

Acknowledgment. D.L.C. and R.J.K. acknowledge the financial support of an Australian Postgraduate Award. This work was also supported by a grant of supercomputer time under the Merit Allocation Scheme from the Australian Partnership for Advanced Computing National Facility.

Supporting Information Available: The geometries of all structures generated in this work and additional benchmarking data. This material is available free of charge via the Internet at http://pubs.acs.org.

References and Notes

(1) Rang, H. P.; Dale, M. M.; Ritter, J. M. In *Pharmacology*, 4th ed; Churchill Livingstone: Edinburgh, 1999; pp 478−480.

(2) For a review of $GABA_A$ and $GABA_C$ receptors, see: Chebib, M.; Johnston, G. A. R. *J. Med Chem.* **2000**, *43*, 1427.

(3) For a review of $GABA_B$ receptors, see: Bowery, N. G.; Enna, S. J. *J. Pharmacol. Exp. Ther*. **2000**, *292*, 2.

(4) For a review of $GABA_A$ receptors see: Krogsgaard-Larsen, P.; Frølund, B.; Jørgensen, F. S.; Schousboe, A. *J. Med. Chem.* **1994**, *37*, 2489.

(5) Drew, C. A.; Johnston, G. A. R.; Weatherby, R. P. *Neurosci. Lett.* **1984**, *52*, 317.

(6) For a review of research into $GABA_C$ receptors, see: Chebib, M. *Clin. Exp. Pharmacol. Physiol.* **2004**, *31*, 800.

(7) Johnston, G. A. R.; Burden, P. M.; Mewett, K. N.; Chebib, M., inventors. University of Sydney and Circadian Technologies, assignees. Patent Number 98:58939, 30 December 1998.

(8) Arnaud, C.; Gauthier, P.; Gottesmann, C. *Psychopharmacology* **2001**, *154*, 415.

(9) Yang, L.; Omori, K.; Omori, K.; Otani, H.; Suzukawa, J.; Inagaki, C. *J. Neurochem.* **2003**, *87*, 791.

(10) Boue-Grabot, E.; Taupignon, A.; Tramu, G.; Garret, M. *Endocrinology* **2000**, *141*, 1627.

(11) Chebib, M.; Vandenberg, R. J.; Froestl, W.; Johnston, G. A. R. *Eur. J. Pharmacol.* **1997**, *329*, 223.

(12) Murata, Y.; Woodward, R. M.; Miledi, R.; Overman, L. E. *Bioorg. Med. Chem. Lett.* **1996**, *6*, 2071.

(13) Chebib, M.; Mewett, K. N.; Johnston, G. A. R. *Eur. J. Pharmacol.* **1998**, *357*, 227.

(14) Krehan, D.; Frølund, B.; Krogsgaard-Larsen, P.; Kehler, J.; Johnston, G. A. R.; Chebib, M. *Neurochem. Int.* **2003**, *42*, 561.

(15) Lorenzini, M. L.; Bruno-Blanch, L,; Estiu, G. L. *Int. J. Quantum Chem.* **1998**, *70*, 1195.

(16) Haworth, N. L.; Bacskay, G. B. *J. Chem. Phys.* **2002**, *117*, 11175.

(17) Illustrations generated using *Gaussview1.0*; Gaussian, Inc.: Pittsburgh, PA, 1997.

(18) Frisch, M. J.; Trucks, G. W.; Schlegel, H. B.; Scuseria, G. E.; Robb, M. A.; Cheeseman, J. R.; Montgomery, Jr., J. A.; Vreven, T.; Kudin, K. N.; Burant, J. C.; Millam, J. M.; Iyengar, S. S.; Tomasi, J.; Barone, V.; Mennucci, B.; Cossi, M.; Scalmani, G.; Rega, N.; Petersson, G. A.; Nakatsuji, H.; Hada, M.; Ehara, M.; Toyota, K.; Fukuda, R.; Hasegawa, J.; Ishida, M.; Nakajima, T.; Honda, Y.; Kitao, O.; Nakai, H.; Klene, M.; Li, X.; Knox, J. E.; Hratchian, H. P.; Cross, J. B.; Bakken, V.; Adamo, C.; Jaramillo, J.; Gomperts, R.; Stratmann, R. E.; Yazyev, O.; Austin, A. J.; Cammi, R.; Pomelli, C.; Ochterski, J. W.; Ayala, P. Y.; Morokuma, K.; Voth, G. A.; Salvador, P.; Dannenberg, J. J.; Zakrzewski, V. G.; Dapprich, S.; Daniels, A. D.; Strain, M. C.; Farkas, O.; Malick, D. K.; Rabuck, A. D.; Raghavachari, K.; Foresman, J. B.; Ortiz, J. V.; Cui, Q.; Baboul, A. G.; Clifford, S.; Cioslowski, J.; Stefanov, B. B.; Liu, G.; Liashenko, A.; Piskorz, P.; Komaromi, I.; Martin, R. L.; Fox, D. J.; Keith, T.; Al-Laham, M. A.; Peng, C. Y.; Nanayakkara, A.; Challacombe, M.; Gill, P. M. W.; Johnson, B.; Chen, W.; Wong, M. W.; Gonzalez, C.; Pople, J. A. *Gaussian 03*, Revision C.02; Gaussian, Inc., Wallingford CT, 2004.

(19) Becke, A. D. *J. Chem. Phys.* **1993**, *98*, 5648.

(20) Becke, A. D. *Phys. Rev. A* **1998**, *38*, 3098.

(21) Lee, B.; Yang, W.; Parr, R. G. *Phys. Rev. B* **1998**, *37*, 785.

(22) Hariharan, P. C.; Pople, J. A. *Theor. Chim. Acta* **1973**, *28*, 213.

(23) Francl, M. M.; Petro, W. J.; Hehre, W. J.; Binkley, J. S.; Gordon, M. S.; DeFrees, D. J.; Pople, J. A. *J. Chem. Phys.* **1982**, *77*, 3654.

(24) Clark, T.; Chandrasekhar, J.; Schleyer, P.v. R. *J. Comput. Chem.* **1983**, *4*, 294.

(25) Krishnan, R.; Binkley, J. S.; Seeger, R.; Pople, J. A. *J. Chem. Phys.* **1980**, *72*, 650.

(26) Gill, P. M. W.; Johnson, B. G.; Pople, J. A.; Frisch, M. J. *Chem. Phys. Lett.* **1992**, *197*, 499.

(27) Frisch, M. J.; Pople, J. A.; Binkley, J. S. *J. Chem. Phys.* **1984**, *80*, 3265.

(28) Pople, J. A.; Binkley, J. S.; Seeger, R. *Int. J. Quantum Chem., Quantum Chem. Symp.* **1976**, *10*, 1.

(29) Krishnan, R.; Pople, J. A. *Int. J. Quantum Chem.* **1978**, *14*, 91.

(30) Bartlett, R. J.; Silver, D. M. *J. Chem. Phys.* **1975**, *62*, 3258.

(31) Bartlett, R. J.; Purvis, G. D. *Int. J. Quantum Chem.* **1978**, *14*, 561.

(32) Klamt, A.; Schuurmann, G. *J. Chem. Soc., Perkin Trans. 2* **1993**, 799.

(33) Barone, V.; Cossi, M.; Tomasi, J. *J. Comput. Chem.* **1998**, *19*, 404.

(34) Crittenden, D. L.; Chebib, M.; Jordan, M. J. T. *J. Phys. Chem. A* **2004**, *108*, 203.

(35) Pople, J. A.; Head-Gordon, M.; Fox, D. J.; Raghavachari, K.; Rassolov, V.; Curtiss, L. A. *J. Chem. Phys.* **1989**, *90*, 5622.

(36) Crittenden, D. L.; Chebib, M.; Jordan, M. J. T. *J. Phys. Chem. A* **2005**, *109*, 4195.